EXPERIMENTAL AND SIMULATION TESTING OF THERMAL LOADING IN THE JET TABS OF A THRUST VECTOR CONTROL SYSTEM

by

Saša Ž. ŽIVKOVIĆ[a*], Momčilo M. MILINOVIĆ[b], Predrag Lj. STEFANOVIĆ[c], Pavle B. PAVLOVIĆ[c], and Nikola I. GLIGORIJEVIĆ[d]

[a] Military Technical Institute, Belgrade, Serbia
[b] Faculty of Mechanical Engineering, University of Belgrade, Belgrade, Serbia
[c] Laboratory for Thermal Engineering and Energy, Vinca Institute for Nuclear Sciences, University of Belgrade, Belgrade, Serbia
[d] Military Technical Institute, Belgrade, Serbia;
Department for Chemical Engineering, Military Academy, Belgrade, Serbia

Original scientific paper
DOI: 10.2298/TSCI150914208Z

The paper discusses the temperature changes in mechanical jet tabs in a system of rocket motor thrust vector control, estimated by the simulation and experimental tests methodology. The heat transfer calculation is based on complex computational fluid dynamics simulations of both the nozzle and external tab flows, as the comprehensive integral flow zones with high flow parameters gradients. Due to a complexity of the model for flow calculations, the experimental estimation of the calculated results is carried out. The temperature is measured by jet tabs embedded thermocouples, and conducted through the rocket motor static tests. A good agreement of the calculated and measured results is achieved. The main aim of the developed method is to establish an approved calculation tool for designing new thurst vector control systems in order to avoid disadvantages due to overheating.

Key words: *thrust vectoring, rocket motor, jet tabs, thermal loading, thermocouples, heat transfer, computational fluid dynamics*

Introduction

Thrust vector control (TVC) system is designed as the executive subsystem of a command guided short range antitank missile. In this case, the most important capability of the missile is its high maneuverability, mainly in the horizontal plane [1]. This performance requires a high rate response control system of the missile. Also, the command forces of flight have to be independent of flight velocity and an actual shooting target distance. These two requirements exclude using aerodynamic control systems, because they strongly depend on flight velocity. Among other TVC system types, a mechanical jet tabs TVC system (fig. 1) has been chosen as the best solution since it has low mass, small size and requires low power actuators. High maneuverability is also achieved using the concept of flight control with command forces generated in the center of the gravity, which maximizes the dynamic response of the missile. The missile has a special design concept (fig. 1) with jet tabs operating in pairs on each nozzle. The tabs deflect the motor jets on the same side, generating dual lateral forces, opposite to the direc-

* Corresponding author; e-mail: sasavite@yahoo.com

tion of the jets deflection. The surfaces of the tabs are plan-parallel to the nozzle exit area surfaces but perpendicular to the jet main stream. The gap between the tabs and the nozzle exit surface exists because of constructive and functional reasons, such as thermal dilatations, particles condensation of the combustion spaces, *etc.* But leaking of the products through this gap decreases the gasdynamic efficiency of the thrust vectoring process.

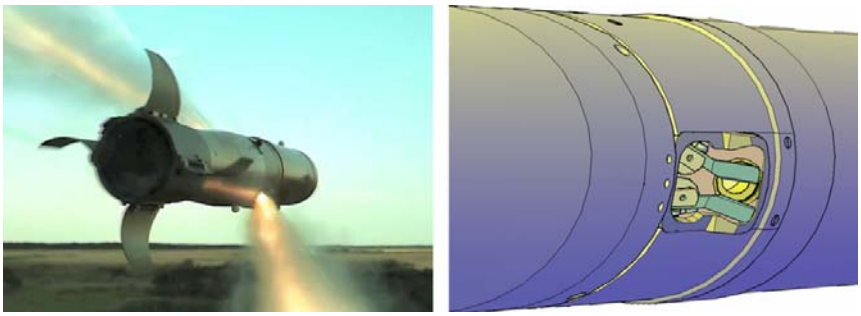

Figure 1. Antitank missile in flight with thrust vectoring (left), and a detail of a mechanical TVC system with the jet tab in the command position (right)

Heat transfer calculations represent one of the most important tasks in the rocket motor (RM) design process. An enormous heat amount is released in a short period of time, in a construction which is limited in mass and volume. The majority of parts of rocket motor systems must be optimized to withstand mechanical and thermal loadings [2]. The design of TVC subsystems realizes the mentioned complex operational flow fields, as a result of comprehensive integral flow zones with high flow parameters gradients, where temperature fields are of the crucial importance for thermal loading predictions. The prediction of temperature changes in the jet tabs provides the first step in the estimation of their thermal loadings as a design requirement.

Recently, there have not been many published research papers in the field of thermo--mechanical analyses of TVC system mechanical elements. This technology was in the focus in the past decades, and recently other TVC system types, such as fluidic thrust vectoring, have had priority [3]. The calculations realized using computational fluid dynamics (CFD) methods by the commercial FLUENT program [4] are shown in the papers [5, 6]. The authors point out a good applicability of the FLUENT program employed on the TVC vane subsystems immersed in the nozzle supersonic flow. The comparative measurements and the CFD simulations in the FLUENT program, employed on this type of TVC configuration, are reported in the papers [7]. Also, some previous papers refer to the experimental measurements of temperature fields in jet vanes using thermocouples [8] or infrared thermography [9], as well as to the development of the heat transfer calculation methods. The main effort in the mentioned experimental supported papers, and in some other research works presented in [10, 11], is to determine the resistance of composite jet vane structures to hot flow erosion. The experience from these research works is very useful in this study, because TVC systems with jet tabs work in similar environmental combustion conditions. The experimental verification in this paper uses a non-scaled geometry model in accordance with the operating conditions of the missile.

Experimental testing equipment

The measurement of temperature changes during the rocket motor test is conducted using thermocouples embedded into the jet tabs. To realize such experiments, two main sub-

systems are composed: the first one is a testing object and the second one is a measurement-acquisition system. The scheme is shown in fig. 2. The main parts of the testing object are the executive elements of a TVC system – jet tabs, integrated with an experimental rocket motor, with operating conditions identical to those in a real missile in order to provide a non-scaled geometry model of the environmental conditions for the tabs. The dynamics of the tabs is excluded and they generate required continual command force in the nozzles. The jet tabs are fixed in the command position in order to estimate threshold thermal loadings in the full rocket engine operation time. An appropriate estimation criterion for the temperature increase is taken for the maximum time cycle of the tabs operation.

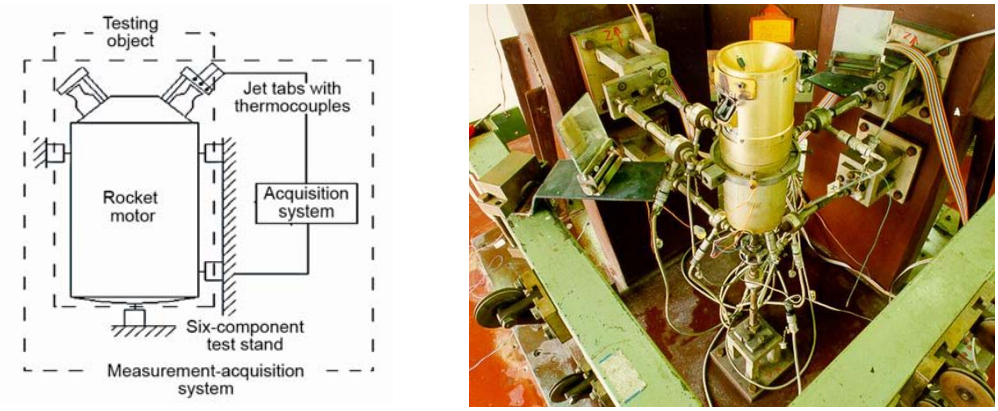

Figure 2. Experimental equipment: a testing object – an RM with jet tabs; the measurement-acquisition system – a six-component test stand, the thermocouples and the acquisition system

The propellant used in the tests generates identical combustion products as in a real RM. For temperature measurements, thermocouple probes are used, with the 0.5 mm outer diameter, taking the small size of the jet tabs into consideration. The probes are embedded into the jet tabs at certain depths, at the back side of the tabs, in the position shown in fig. 3. This position is chosen to avoid possible damage to the thermocouple wires with the motor jets. Also, the probes are fixed in this position using a special shield.

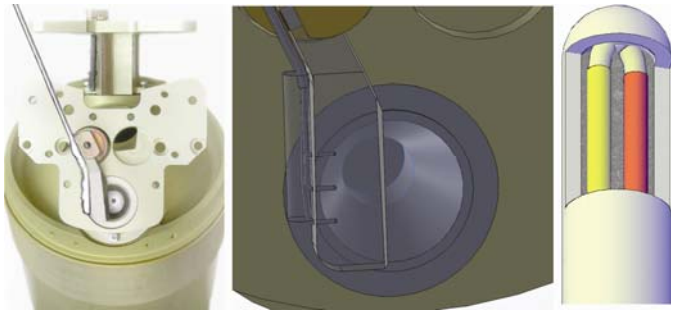

Figure 3. Testing object – a jet tab with the embedded thermocouples, in the command position (left). A detail with the exact location of the measuring points (middle). Small diameter probe with type K thermocouple, grounded in protective sheath design (right)

The probes consist of type K thermocouples, a Nickel-Chromium/Nickel-Alumel combination, in a coaxial grounded construction. The thermocouple wires are protected with *inconel* 600 sheathing (fig 3). The empty space in the sheath is filled with magnesium oxide

(MgO) powder insulation for the mechanical and thermal protection of the thermocouple wires. This probe design allows a fast response time because the hot junction of the thermocouple has a direct contact to the outside environment.

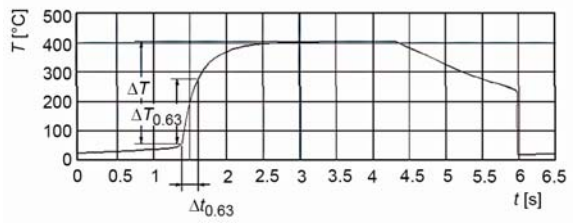

Figure 4. Thermocouple dynamic response determination diagram

Time constant of the thermocouples is defined as dynamic response on temperature shock. Thermocouple signals are measured after fast inserting of probe into measuring hole, in calibration jet tab which is preheated at $T \approx 400$ °C. Analyzing recorded temperature-time curve, shown in fig. 4, time constant $\Delta t_{0.63} = 0.21$ s is determined, as time period necessary for reaching of 63% of chosen referent temperature range $\Delta T = 380$ °C. This time constant enables chosen thermocouples to accurately measure fast temperature changes, with frequency les then $f_T < 10\Delta t_{0.63} = 2.1$ Hz. Estimated frequency of process of jet tabs heating, during RM operation cycle, is around $f_T \approx 0.25$ Hz.

The applied acquisition system has a sufficient number of channels, for six load cells and six thermocouples, fig. 2.

Heat transfer simulation test on the jet tabs

The convective heat transfer of combustion products is the dominant heat exchange process on the jet tabs. For this reason, a key factor in precise heat transfer calculations is an accurate simulation of the combustion product flow through the RM domain as well as through the nozzles and in the zone of the TVC system executive elements. Simultaneously, the most complicated product flow process occurs in this zone. The commercial FLUENT software is chosen for this calculation, because it is suitable for solving this type of problems, and has post processing tools which enable the extraction of temperature changes as data in the chosen points of the jet tabs. The calculation is conducted in an unsteady simulation of all important processes in the experiment. All heat transfer processes in the simulation are calculated simultaneously with the product flow processes. The parameters of these processes and the material characteristics used in the simulations are defined and tested in the described numerical model.

Simulations of a combustion product flow

The simulation model of a combustion product flow consisted of the experimental RM parameters as well as flow domain geometry, internal ballistic operating regime, thermochemical characteristics of combustion products and turbulent characteristics of the internal RM flow. Each of them is considered in the next text.

Flow domain geometry model

Flow domain geometry model of the RM and TVC system components internal/external space is reproduced by the grid program performances (fig. 3). This geometrical shape has strong influence on the product flow, and, consequently the grid shape design has to be precise. The main influential geometry parameters on the TVC process effects are: percentage of the covered part of the exit nozzle plane with the jet tab (shadowed ratio), distance

between the nozzle exit plane and the jet tab surface (tab gap), nozzle expansion ratio and nozzle divergence angle [12].

Internal ballistic operating regime

This regime determines the flow total pressure was extracted from the RM static test results as a parameter measured in the parallel experimental tests described in this paper, as well as in the previous similar tests given in the paper [13]. This parameter is introduced in the calculation as a flow inlet boundary condition. The additional measured RM thrust components are also simulated numerically and are used as parameters for the control of the calculation accuracy.

Thermo-chemical characteristics

Thermo-chemical characteristics necessary for this calculation, are the combustion process and the physical characteristics of combustion gaseous products (fig. 5):

- estimated combustion temperature $T_c = 2300$ K,
- molecular weight $M = 23.5$ kg/kmol,
- specific heat capacity – c_p,
- thermal conductivity – k, and
- dynamic viscosity – μ.

All these characteristics are obtained using the thermo-chemical calculation of the combustion products frozen flow presented in [14, 15]. The products are considered to be an ideal gas.

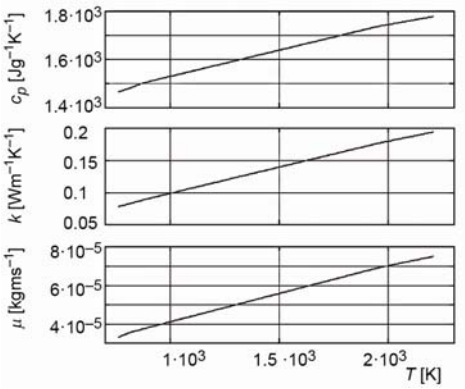

Figure 5. Thermo-physical characteristics of the combustion products – specific heat, thermal conductivity and dynamic viscosity

Turbulent characteristics

Turbulent characteristics of the internal RM flow are modeled using the transition SST turbulence model [4]. This model is chosen considering the previous tests in this research presented in the paper [12]. The turbulent intensity value [4] is:

$$I = 0.16\ \mathrm{Re}^{-1/8} \tag{1}$$

where Re is the Reynolds number of the product flow, which can be calculated by a semiempirical equation for combustion chamber conditions [16]:

$$\mathrm{Re} = \frac{3.46 D_t p_c}{\mu\sqrt{R_g T_c}} \tag{2}$$

with the parameters determined by: D_t – the RM throat diameter, p_c – the chamber pressure, and R_g – the specific gas constant of the products in the combustion chamber and for the nozzle inlet (fig. 6). The diameter of the inlet tube of the nozzle is chosen as a hydraulic diameter value [4]. The intermittency factor is taken to be 1, because in a fully turbulent nozzle inlet flow, or at least transient, a boundary layer regime is achieved [4].

The CFD model, with the described input data, determines the product flow parameters such as: velocity, pressure, temperature, density, turbulence parameters, *etc.* (fig. 6). A

detailed mathematical model of calculation is described in the FLUENT literature [4] as well as in the previous research in the paper [12].

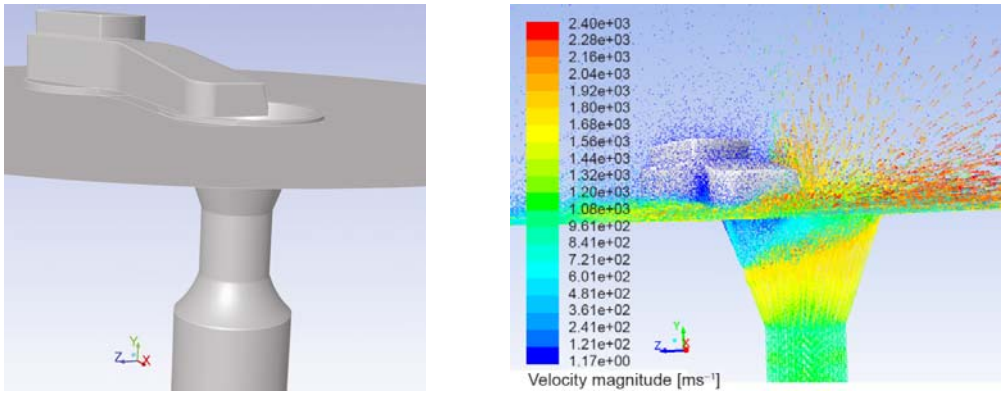

Figure 6. The CFD geometry model: the RM nozzle and the TVC system parts – the tab in the working position and the deflector plate (left) product flow velocity vector field (right)

The profiles of temperature of the products stream through the nozzle and exterior are shown in fig. 7. The static temperature of the total flow field is shown without jet deflection (left), and with jet tab deflection (right). This flow field has a crucial impact on the heat transfer process on the tabs in the process of their thermal loading definition.

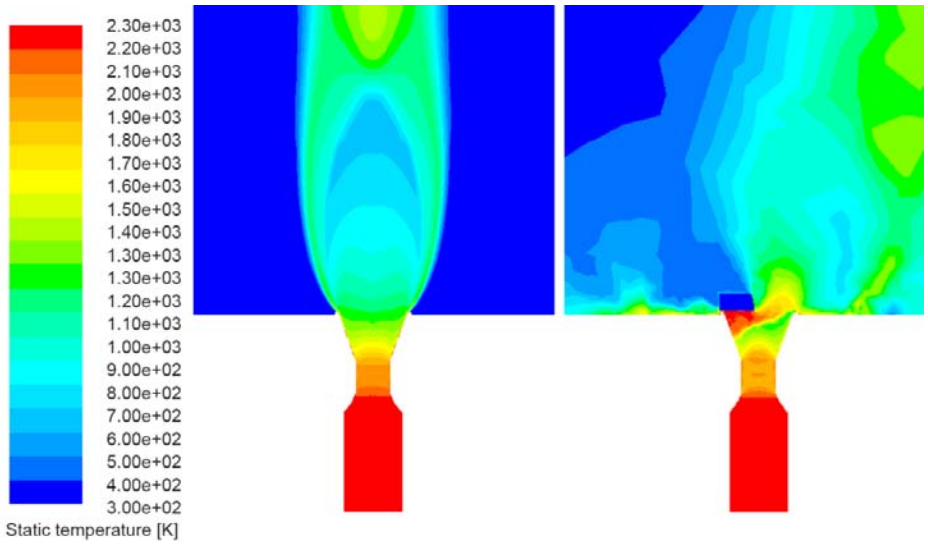

Figure 7. Profiles of the static temperature of combustion products, in the axial direction nozzle plane cross-section, without (left), and with jet tab deflection (right)

The re-circulation zone, formed by a jet tab insertion, is presented in fig. 7. The product flow velocity in this zone is low and the static temperature approaches the total tem-

perature. Figure 8 shows the curves of the static temperature in the nozzle exit plane, in both models, with and without jet deflection. The value of the temperature of products, in the re-circulation zone upstream of the jet tab, is close to the total temperature. This zone is the main heat source of jet tab thermal loading.

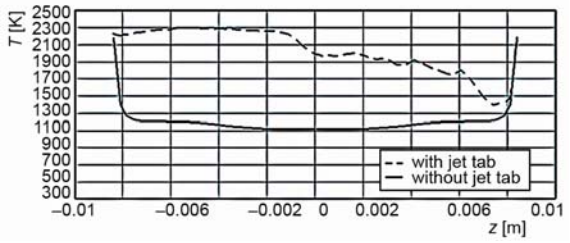

Figure 8. Distribution of the static temperature of combustion products, in the nozzle exit plane, without and with jet tab deflection

Simulation of heat transfer and thermal loading

The amount of heat released in a combustion process primarily depends on propellant characteristics. Combustion temperature is a dominant factor in the heat transfer process and it also has a strong influence on flow parameters, flow velocity in particular. Three types of heat transfer are present in the RM operation: conductive, convective and radiative. All types are the result of combustion product evolution in RM and their internal flow.

Conduction

Conduction process is estimated comprehensively by the energy equation, used in FLUENT, for a solid material of an accepted geometry, in the form:

$$\frac{\partial}{\partial t}(\rho h) = \nabla(k\nabla T) \tag{3}$$

Change in time of the enthalpy h and density ρ product, for each cell of the software calculating grid, within the calculating domain, is dependent on temperature gradients and material thermal conductivity. At a current temperature T, enthalpy is calculated as an integral of material specific heat change from the referent temperature taken as $T_{\text{ref}} = 298.15$ K, *i. e.*:

$$h = \int_{T_{\text{ref}}}^{T} c_{\text{p}}\,\mathrm{d}T \tag{4}$$

Convection

Convection is a more complex process then conduction. It mainly depends on fluid and solid material thermo-dynamic properties, similarly to a conduction process, as well as on local fluid flow parameters around a solid body and its temperature. As previously mentioned, CFD methods enable a precise calculation of flow and turbulence parameters in boundary layers, which is necessary for calculating the convection coefficient. Convective heat transfer from a fluid region on a solid tab is calculated as equilibrium of the heat fluxes from both sides, fluid and solid, respectively:

$$q = h_{\text{f}}(T_{\text{w}} - T_{\text{f}}) \tag{5}$$

$$q = \frac{k_{\text{s}}}{\Delta n}(T_{\text{w}} - T_{\text{s}}) \tag{6}$$

where h_{f} is the convective heat transfer coefficient; T_{w}, T_{f}, and T_{s} are the temperatures at the wall surface, calculating the cell centers in fluid and solid sides, respectively; k_{s} is the thermal

conductivity of the solid material, and Δn – the distance between the wall surface and the solid cell center.

With the obtained temperature profiles in the flow field, turbulent and other flow characteristics, eqs. (5) and (6), the fluid-side heat transfer coefficient k_f is calculated by Fourier's law, applied on the walls:

$$q = k_f \left(\frac{\partial T}{\partial n} \right)_{wall} \tag{7}$$

where n is the local co-ordinate normal to the wall.

Solid material heat conduction process is dependent on material properties, such as thermal conductivity, specific heat capacity, and density. The first two characteristics are given as a function of temperature for molybdenum, as a jet tabs material (fig. 9) [17].

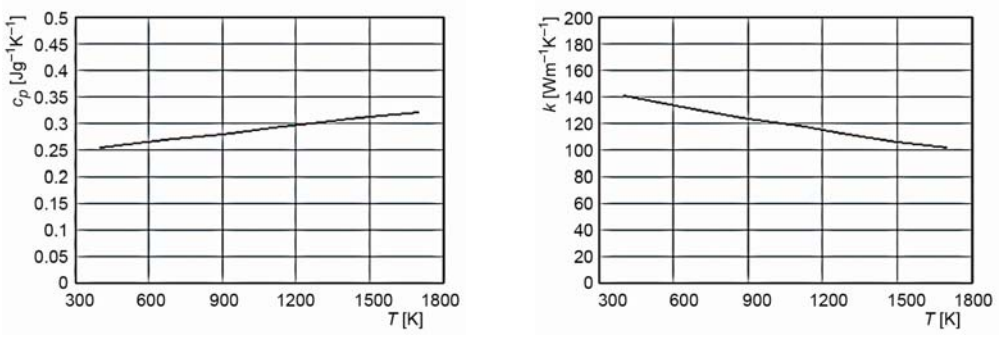

Figure 9. Molybdenum thermal properties: the curves of specific heat and thermal conductivity *vs.* temperature

Radiation

The P-1 heat radiation model is also applied. The radiation heat flux at the walls of the jet tab is calculated by the equation:

$$q_r = -\frac{\varepsilon_w}{2(2-\varepsilon_w)}(4\sigma T_w^4 - G_w) \tag{8}$$

where ε_w is the emissivity of the wall surfaces, σ – the Stefan-Boltzmann constant, and G_w – the incident radiation.

The optical thickness of the products is near 1, and the P-1 is a recommended model for this case [4]. The inlet tube of the flow nozzle in a real RM has a small volume, so the quantity of hot gas, as a source of the radiation, is also small. The largest source of radiation is the inlet surface of the tube. Hot products from the combustion chamber radiate through the inlet tube and the nozzle throat in the axis direction (figs. 2 and 7). The small part of the tab is irradiated by this source of heat, and consequently, a small contribution of radiation in the total heat flux is expected. FLUENT enables a separated calculation of radiation and total heat flux. A comparison in several time steps shows that radiation heat flux is lower than a few percent, so radiation heat flux can be neglected.

Comparative analysis and the discussion of the results

A simulated temperature distribution on the jet tab surfaces is presented in fig. 10, occurring one second after the flow initiation from the domain inlet. The shadowed part of the

jet tab is heated most intensely (left projection in fig. 10) and the temperature reaches the highest level. The temperature increase in the tabs depth is speeded up by conduction in all directions (center projection). Due to the large temperature gradients in the tab, after a second interval of localized overheating, the temperature increases significantly along the whole jet tab length (right projection).

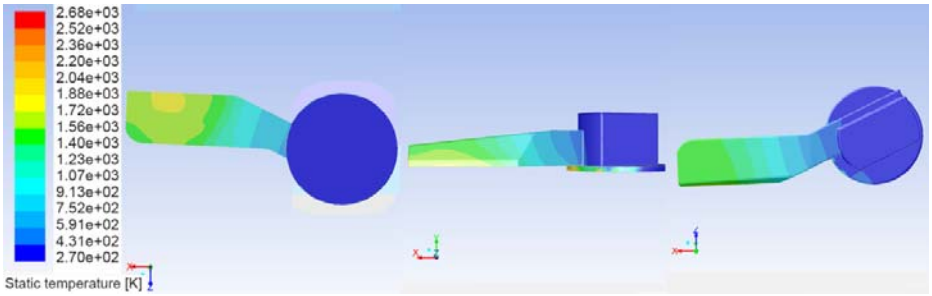

Figure 10. Temperature distribution contours on the jet tab surfaces, one second after the RM ignition

Figure 11 shows the temperature distribution in the flow domain and the jet tab depth, in two perpendicular section planes in the first second. In the vicinity of solid surfaces (the jet tab and the nozzle walls) large gradients of temperature can be noticed. The gradients are positive in the shadowed part of the tab, and negative in the other parts of the tab, because the flow temperature is lower than the temperature of the tab.

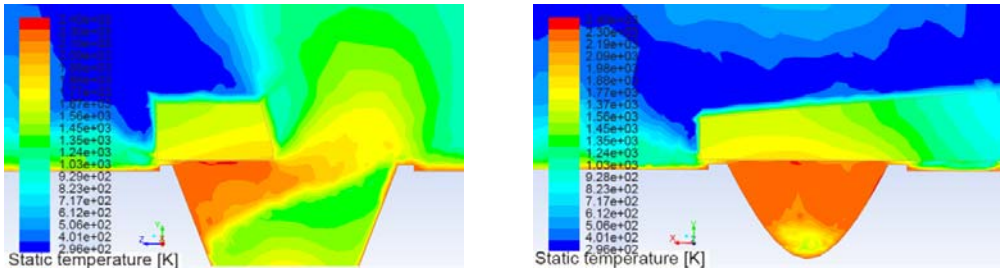

Figure 11. Temperature distribution in the flow domain and the jet tab cross section (left) and the longitudinal section (right), one second after the RM ignition

FLUENT calculates the local heat transfer coefficient at each part of the solid surfaces, and its distribution is shown in fig. 12, left. The highest value of the coefficient is localized in the junction zone of the tab and its support, where the flow velocity of the products is highest. The heat flux distribution is shown in fig. 12, right. The highest values of the heat flux are in the shadowed part of the tab, due to the largest temperature difference, as well as in the junction zone where the heat transfer coefficient is largest.

In fig. 13, the temperature changes at the measurements points are shown as temperature-time curves, obtained in the experiment and the CFD simulation. A good agreement can be noticed comparing the experimental results with the calculated ones. This agreement can be considered as a verification of the applied CFD calculation method for this type of heat transfer problems.

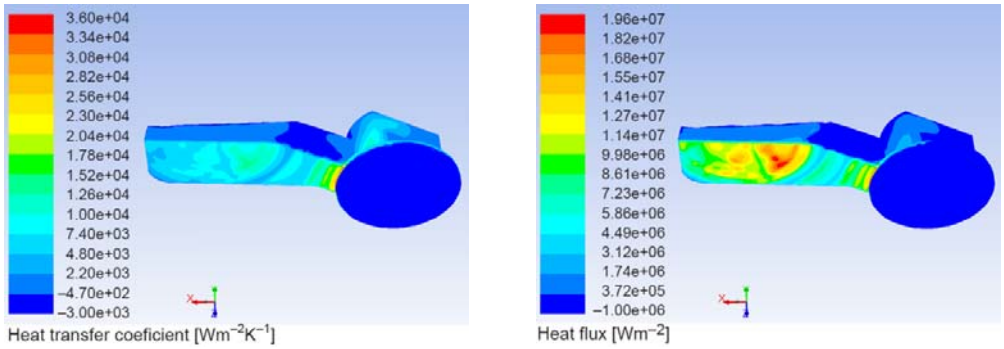

Figure 12. Heat transfer coefficient (left) and heat flux distribution (right) contours on the jet tab surfaces, one second after the RM ignition

In all parts of the tab, a high level of temperature is reached very fast. Consequently, the mechanical characteristics of the jet tab significantly decrease. The research work [18] has pointed out a drastic reduction in molybdenum strength with temperature increase. At high temperatures over 1000 K, the tensile strength of molybdenum decreases almost four times. It is expected that the jet tab bends under gasdynamic force.

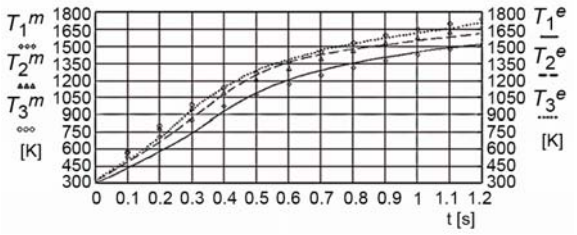

Figure 13. Measurement points temperatures-time curves, comparison of the experimental T^e and the CFD simulation model T^m

The effect of this deformation can be noticed indirectly, analyzing the diagrams of the RM thrust components (fig. 14). The axial component of the thrust Fa is slightly increasing. The side force Fb reaches a peak at first, then remains approximately constant until 0.4 second, when it begins slightly to decrease. The relative side force B (side force relativized with undisturbed thrust F), has a similar character to the side force, but it has a more obvious decreasing. The influence of the jet tab gap on the thrust vectoring efficiency is described in [12]. The relative side force drastically decreases with the tab gap increase. The deformation of the tab leads to the gap increase and, consequently, to the relative side force decrease. This effect can be noticed on the diagram of the measured thrust components (fig. 14).

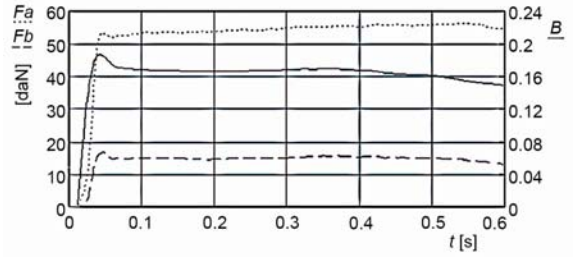

Figure 14. Six-component test stand results: axial thrust component F_a, side force F_b and relative side force B *vs.* time t diagrams

Conclusions

A calculation method using a CFD simulation is developed in order to determine the temperature fields and thermal loading of mechanical TVC system jet tabs. The verification of

the CFD method is carried out by the measurement of temperature changes, using thermocouples embedded in discrete points in the tabs material. The comparison of the CFD simulation and experimental results has shown that the developed calculation method is accurate enough to provide necessary estimations for the thermal loading calculation in the design of new similar solutions. With the estimated temperature field, jet tabs should be designed optimally to withstand mechanical and thermal stresses during the process of hot gas flow and the generation of required lateral forces.

The developed method of temperature measurement was partially successful. The temperature in the tabs reached 2000 K, under the condition of strong gasdynamic forces caused by strong secondary jets of RM combustion products. The applied thermocouples were not functional during the full RM operation cycle; however, they satisfied the required jet tabs measurement cycle. The threshold temperature loading in the measurement experiments was an expected monitored effect of thermal loading on the RM, inflicting reactive side force degradation caused by the deformation of components [2]. The threshold temperature loading in the measurement experiments was an expected monitored effect of thermal loading on the RM, inflicting reactive side force degradation caused by the deformation of TVC components. The main disadvantage of the applied TVC type is this effect, expressed in the form of efficiency decrease, increased thrust loss and decreased lateral force during operation [2]. Further research should concentrate on thermocouples with higher resistance such as the probes capable of covering the whole RM combustion process. Better materials of the jet tabs support are also necessary, in order to avoid the whole construction deformation as well as additional jet gap increase and gas flow leaking.

Acknowledgments

This paper is the part of the research on the project III47029 of MPN TR RS.

Nomenclature

B – relative side force, ($=F_b/F$), [–]
c_p – specific heat capacity, [$Jkg^{-1}K^{-1}$]
D_t – RM throat diameter, [m]
F – thrust, [N]
F_a – axial component of thrust, [N]
F_b – side force, [N]
f_T – frequency of temperature change, [Hz]
G_w – incident radiation, [Wm^{-2}]
h – enthalpy, [Jkg^{-1}]
h_f – convective heat transfer coefficient, [$Wm^{-2}K^{-1}$]
I – turbulent intensity, [%]
k – thermal conductivity, [$Wm^{-1}K^{-1}$]
M – molecular weight, [$kgkmol^{-1}$]
n – normal direction, [m]
p – pressure, [Pa]
q – heat flux, [Wm^{-2}]
Re – Reynolds number, [–]
Rg – specific gas constant, ($=R/M$), [$Jkg^{-1}K^{-1}$]
T – temperature, [K]
t – time, [s]

Subscripts

c – chamber
f – fluid
r – radiation
ref – referent
s – solid
w – wall

Greek symbols

Δ – period, [–]
ε – emissivity, [–]
μ – dynamic viscosity, [$kgm^{-1}s^{-1}$]
ρ – density, [kgm^{-3}]
σ – Stefan-Boltzmann constant, ($5.670373\cdot10^{-8}$), [$kgs^{-3}K^{-4}$]

Acronymus

CFD – computational fluid dynamics
RM – rocket motor
TVC – thrust vector control

References

[1] Ocokoljić, G., *et al.*, Aerodynamic Coefficients Determination for Antitank Missile with Lateral Jets, *Proceedings*, 4th International Scientific Conference on Defensive Technologies OTEH, Belgrade, 2011, pp. 17-22

[2] Maw, J. F., *et al.*, Verification of RSRM Nozzle Thermal Models with ETM-3 Aft Exit Cone In-depth Temperature Measurements, *Proceedings*, 40th AIAA/ASME/SAE/ASEE Joint Propulsion Conference and Exhibit, Fort Lauderdale, Fla., USA, 2004
[3] Gal-Or, B., Fundamental Concepts of Vectored Propulsion, *Journal of Propulsion and Power, 6* (1990), 6, pp. 747-757
[4] ***, Fluent Inc., FLUENT 5 User's Guide, 1998
[5] Yu, M. S., *et al.*, Hybrid Method for Jet Vane Thermal Analysis in Supersonic Nozzle, *Journal of Thermo Physics and Heat Transfer*, *20* (2006), 3, pp. 402-409
[6] Rainville, P. A., *et al.*, Unsteady CFD Calculation for Validation of a Multi-Vane Thrust Vector Control System, *Proceedings*, 40th AIAA/ASME/SAE/ASEE Joint Propulsion Conference and Exhibit, Fort Lauderdale, Fla., USA, 2004
[7] Rainville, P. A., *et al.*, CFD Validation with Measured Temperatures and Forces for Thrust Vector Control, *Proceedings*, 38th AIAA/ASME/SAE/ASEE Joint Propulsion Conference and Exhibit, Fort Lauderdale, Fla., USA, 2002
[8] Danielson, A. O., Driels, M. R., Testing and Analysis of Heat Transfer in Materials Exposed to Non-Metallized HTPB Propellant, Department of Mechanical Engineering, Naval Postgraduate School, Monterey, Cal., USA, 1992
[9] Spence, M. T., Applications of Infrared Thermography in Convective Heat Transfer, Ph. D. thesis, Naval Postgraduate School, Monterey, Cal., USA, 1986
[10] Gardner, R. S., Erosion Effects on TVC Vane Heat Transfer Characteristics, Ph. D. thesis, Naval Postgraduate School, Monterey, Cal., USA, 1994
[11] Nunn, H. R., TVC Jet Vane Thermal Modeling Using Parametric System Identification, Naval Postgraduate School, Monterey, Cal., USA, 1988
[12] Živković, S., *et al.*, Tunnel Tests and Numerical Simulation of the High Speed Separated Nozzle Flow, *FME Transactions*, *42* (2014), 3, pp. 89-97
[13] Živković, S., *et al.*, Experimental Determination of Rocket Motor Internal Ballistic Coefficients and Performance Parameters, *Proceedings*, 6th International Scientific Conference on Defensive Technologies OTEH, Belgrade, 2014
[14] Filipović, M., Kilibarda, N., Calculation of Complex Chemical Equilibrium Compositions of Composite Rocket Propellants Combustion Products, *J. Serb. Chem. Soc*., *65* (2000), 11, pp. 803-810
[15] Živković, S., *et al.*, Solid Propellant Rocket Motor Nozzle Heat Transfer Model Verification, *Proceedings*, 5th International Scientific Conference on Defensive Technologies OTEH, Belgrade, 2012, pp. 350-354
[16] Dobrovolskii, V. M., Liquid Rocket Engines (in Russian), Mashinostroenie, Moscow, 1968
[17] ***, Plansee Group, http://www.plansee.com/en/Materials-Molybdenum-402.htm
[18] ***, Delft University of Technology, http://www.lr.tudelft.nl/organisatie/afdelingen/space-engineering/space-systems-engineering/expertise-areas/space-propulsion/design-of-elements/design-and-analysis-data/properties-of-specific-structural-materials-used-for-rocket-motors/

Paper submitted: September 14, 2015
Paper revised: December 1, 2015
Paper accepted: December 2, 2015